

# ON SURFACE MESHES INDUCED BY LEVEL SET FUNCTIONS

MAXIM A. OLSHANSKII\*, ARNOLD REUSKEN†, AND XIANMIN XU‡

**Abstract.** The zero level set of a continuous piecewise-affine function with respect to a consistent tetrahedral subdivision of a domain in  $\mathbb{R}^3$  is a piecewise-planar hyper-surface. We prove that if a family of consistent tetrahedral subdivisions satisfies the *minimum angle condition*, then after a simple postprocessing this zero level set becomes a consistent surface triangulation which satisfies the *maximum angle condition*. We treat an application of this result to the numerical solution of PDEs posed on surfaces, using a  $P_1$  finite element space on such a surface triangulation. For this finite element space we derive optimal interpolation error bounds. We prove that the diagonally scaled mass matrix is well-conditioned, uniformly with respect to  $h$ . Furthermore, the issue of conditioning of the stiffness matrix is addressed.

**Key words.** surface finite elements, level set function, surface triangulation, maximum angle condition

**1. Introduction.** Surface triangulations occur in, for example, visualization, shape optimization, surface restoration and in applications where differential equations posed on surfaces are treated numerically. Hence, properties of surface triangulations such as shape regularity and angle conditions are of interest. For example, angle conditions are closely related to approximation properties and stability of corresponding finite elements [1, 2].

In this article, we are interested in the properties of a surface triangulation if one considers the zero level of a continuous piecewise-affine function with respect to a consistent tetrahedral subdivision of a domain in  $\mathbb{R}^3$ . The zero level of a piecewise-affine function is a piecewise-planar hyper-surface consisting of triangles and quadrilaterals. Each quadrilateral can be divided into two triangles in such a way that the resulting surface triangulation satisfies the following property proved in this paper: if the volume tetrahedral subdivision satisfies a minimum angle condition, then the corresponding surface triangulation satisfies a maximum angle condition. We show that the maximum angle occurring in the surface triangulation can be bounded by a constant  $\phi_{\max} < \pi$  that depends only on a stability constant for the family of tetrahedral subdivisions.

The paper also discusses a few implications of this property for the numerical solution of surface partial differential equations. Numerical methods for surface PDEs are studied in e.g., [6, 4, 5, 3, 8, 10]. We derive optimal approximation properties of  $P_1$  finite element functions with respect to the surface triangulation and a uniform bound for the condition number of the scaled mass matrix. We also show that the condition number of the (scaled) stiffness matrix can be very large and is sensitive to the distribution of the vertices of tetrahedra close to the surface. Some numerical examples illustrate the analysis of the paper.

**2. Surface meshes induced by regular bulk triangulations.** Consider a smooth surface  $\Gamma$  in three dimensional space. For simplicity, we assume that  $\Gamma$  is connected and has no boundary. Let  $\Omega \subset \mathbb{R}^3$  be a bulk domain which contains

---

\*Department of Mathematics, University of Houston, Houston, Texas 77204-3008 and Dept. Mechanics and Mathematics, Moscow State University, Moscow 119899 (molshan@math.uh.edu).

†Institut für Geometrie und Praktische Mathematik, RWTH-Aachen University, D-52056 Aachen, Germany (reusken@igpm.rwth-aachen.de, xu@igpm.rwth-aachen.de).

‡LSEC, Institute of Computational Mathematics and Scientific/Engineering Computing, NCMIS, AMSS, Chinese Academy of Sciences, Beijing 100190, China (xmxu@lsec.cc.ac.cn).

$\Gamma$ . Let  $\{\mathcal{T}_h\}_{h>0}$  be a family of tetrahedral triangulations of the domain  $\Omega$ . These triangulations are assumed to be regular, consistent and stable, cf. [2]. To simplify the presentation, we assume that this family of triangulations is *quasi-uniform*. The latter assumption, however, is not essential for our analysis.

We assume that for each  $\mathcal{T}_h$  an approximation of  $\Gamma$ , denoted by  $\Gamma_h$ , is given which is a connected  $C^{0,1}$  surface without boundary. In our analysis we assume  $\Gamma_h$  to be consistent with  $\mathcal{T}_h$  in the sense as explained in the following definition.

**DEFINITION 2.1.** *For any tetrahedron  $S_T \in \mathcal{T}_h$  such that  $\text{meas}_2(S_T \cap \Gamma_h) > 0$  define  $T = S_T \cap \Gamma_h$ . If every  $T$  is a planar, then the surface approximation  $\Gamma_h$  is called consistent with the outer triangulation  $\mathcal{T}_h$ .*

If  $\Gamma_h$  is consistent with  $\mathcal{T}_h$ , then every segment  $T = S_T \cap \Gamma_h$  is either a triangle or a quadrilateral. Each quadrilateral segment can be divided into two triangles, so we may assume that every  $T$  is a triangle.

Let  $\mathcal{F}_h$  be the set of all triangular segments  $T$ , then  $\Gamma_h$  can be decomposed as

$$\Gamma_h = \bigcup_{T \in \mathcal{F}_h} T. \quad (2.1)$$

**ASSUMPTION 2.1.** *In the remainder of this paper we assume that  $\Gamma_h$  is a connected  $C^{0,1}$  surface without boundary that is consistent with the outer triangulation  $\mathcal{T}_h$ .*

The most prominent example of such a surface triangulation is obtained in the context of level set techniques. Assume that  $\Gamma$  is represented as the zero level of a level set function  $\phi$  and that  $\phi_h$  is a continuous linear finite element approximation on the outer tetrahedral triangulation  $\mathcal{T}_h$ . Then if we define  $\Gamma_h$  to be the zero level of  $\phi_h$  then  $\Gamma_h$  consists of piecewise planar segments and is consistent with  $\mathcal{T}_h$ . As an example, consider a sphere  $\Gamma$ , represented as the zero level of its signed distance function. For  $\phi_h$  we take the piecewise linear nodal interpolation of this distance function on a uniform tetrahedral triangulation  $\mathcal{T}_h$  of a domain that contains  $\Gamma$ . The zero level of this interpolant defines  $\Gamma_h$  and is illustrated in Fig. 2.1.

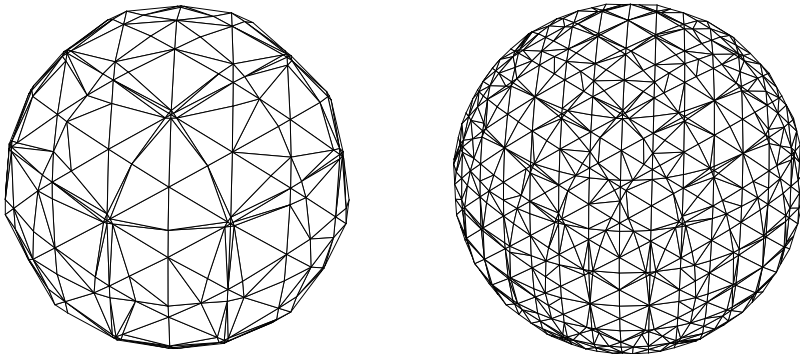


FIG. 2.1. Approximate interface  $\Gamma_h$  for an example of a sphere, resulting from a coarse tetrahedral triangulation (left) and after one refinement (right).

In the setting of level set methods, such surface triangulations induced by a finite element level set function on a regular outer tetrahedral triangulation are very natural and easy to construct. A surface triangulation  $\Gamma_h$  that is consistent with the outer triangulation may be the result of another method than the level set method. In the

remainder we only need that  $\Gamma_h$  is consistent with the outer triangulation and not that it is generated by a level set technique.

Note that the triangulation  $\mathcal{F}_h$  is *not* necessarily regular, i.e. elements  $T \in \mathcal{F}_h$  may have *very small inner angles* and the *size of neighboring triangles can vary strongly*, cf. Fig. 2.1. In the next section we prove that, provided each quadrilateral is divided into two triangles properly, the induced surface triangulation is such that the *maximal angle condition* [1] is satisfied.

**3. The maximal angle condition.** The family of outer tetrahedral triangulations  $\{\mathcal{T}_h\}_{h>0}$  is assumed to be regular, i.e., it contains no hanging nodes and the following stability property holds:

$$\sup_{h>0} \sup_{S \in \mathcal{T}_h} \rho(S)/r(S) \leq \alpha < \infty, \quad (3.1)$$

where  $\rho(S)$  and  $r(S)$  are the diameters of the smallest ball that contains  $S$  and the largest ball contained in  $S$ , respectively. The stability property implies that the family of tetrahedral triangulations satisfies a *minimum* (and thus also maximum) *angle condition*: there exists  $\theta_{\min} > 0$  with

$$\frac{\pi}{2} > \theta_{\min} \geq c(\alpha) > 0, \quad (3.2)$$

such that all inner angles of all sides of  $S \in \mathcal{T}_h$  and all angles between edges of  $S$  and their opposite side are in the interval  $[\theta_{\min}, \pi - \theta_{\min}]$ . The constant  $c(\alpha)$  depends only on  $\alpha$  from (3.1).

Although the surface mesh  $\Gamma_h$  induced by  $\mathcal{T}_h$  can be highly shape irregular, the following lemma shows that a *maximum angle* property holds.

LEMMA 3.1. *Assume an outer triangulation  $\mathcal{T}_h$  from the regular family  $\{\mathcal{T}_h\}_{h>0}$  and let  $\Gamma_h$  be consistent with  $\mathcal{T}_h$ . There exists  $\phi_{\min} > 0$ , depending only on  $\alpha$  from (3.1), such that for every  $S \in \mathcal{T}_h$  the following holds:*

a) *if  $T = S \cap \Gamma_h$  is a triangular element, then*

$$0 < \phi_{i,T} \leq \pi - \phi_{\min} \quad i = 1, 2, 3, \quad (3.3)$$

*holds, where  $\phi_{i,T}$  are the inner angles of the element  $T$ .*

b) *if  $T = S \cap \Gamma_h$  is a quadrilateral element, then*

$$\phi_{i,T} \geq \phi_{\min}, \quad i = 1, 2, 3, 4, \quad (3.4)$$

*holds, where  $\phi_{i,T}$  are the inner angles of the element  $T$ .*

*Proof.* Let  $\theta_{\min}$  be the minimal angle bound from (3.2). Take  $S \in \mathcal{T}_h$ .

We first treat the case where  $T = S \cap \Gamma_h$  is a triangle  $T = BCD$ , as illustrated in Fig. 3.1. Consider the angle  $\phi := \angle BCD$ . Then either  $\phi \leq \pi - \theta_{\min}$  and (3.3) is proved with  $\phi_{\min} = \theta_{\min}$  or  $\phi \in (\pi - \theta_{\min}, \pi)$ . Hence, we treat the latter case. Note that

$$\frac{|CF|}{|AC|} = \sin(\angle CAF) \geq \sin \theta_{\min}$$

and  $\angle BDC < \pi - \phi < \theta_{\min} < \frac{\pi}{2}$ . Take  $E$  on the line through  $DB$  such that  $CE \perp DB$ , and  $F$  in the plane through  $ABD$  such that  $CF$  is perpendicular to this plane. Hence,

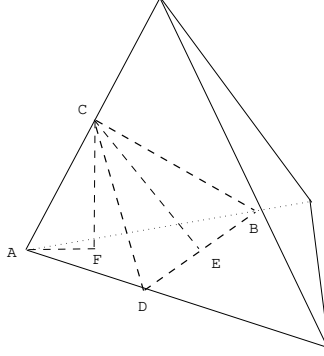


FIG. 3.1.

$|CF| \leq |CE|$  holds. Using the sine rule we get

$$\begin{aligned} \sin(\angle ADC) &= \frac{|AC|}{|CD|} \sin(\angle CAD) \leq \frac{|AC|}{|CD|} \leq \frac{1}{\sin \theta_{\min}} \frac{|CF|}{|CD|} \leq \frac{1}{\sin \theta_{\min}} \frac{|CE|}{|CD|} \\ &= \frac{1}{\sin \theta_{\min}} \sin(\angle BDC) \leq \frac{\sin(\pi - \phi)}{\sin \theta_{\min}} = \frac{\sin(\phi)}{\sin \theta_{\min}} < 1. \end{aligned}$$

Hence,  $\angle ADC \leq \arcsin\left(\frac{\sin \phi}{\sin \theta_{\min}}\right) \leq 2\frac{\sin \phi}{\sin \theta_{\min}}$  holds. This yields

$$\angle ADB < \angle ADC + \angle CDB \leq 2\frac{\sin \phi}{\sin \theta_{\min}} + \pi - \phi.$$

With the same arguments we obtain

$$\angle ABD \leq 2\frac{\sin \phi}{\sin \theta_{\min}} + \pi - \phi.$$

Since  $\angle DAB \leq \pi - \theta_{\min}$  and  $\angle DAB = \pi - (\angle ADB + \angle ABD)$  we get

$$\theta_{\min} \leq 4\frac{\sin \phi}{\sin \theta_{\min}} + 2\pi - 2\phi =: g(\phi). \quad (3.5)$$

Since  $\phi \in (\pi - \theta_{\min}, \pi) \subset (\frac{1}{2}\pi, \pi)$  it suffices to consider  $g(\phi)$  for  $\phi \in (\frac{1}{2}\pi, \pi)$ . Elementary computation yields  $g(\frac{1}{2}\pi) > \theta_{\min}$ ,  $g(\pi) = 0$  and  $g$  is monotonically decreasing on  $(\frac{1}{2}\pi, \pi)$ . Hence the inequality (3.5) holds iff  $\phi \leq \phi_0$ , where  $\phi_0$  is the unique solution in  $(\frac{1}{2}\pi, \pi)$  of  $g(\phi) = \theta_{\min}$ . This proves the result in a).

We now consider the case where  $T = S \cap \Gamma_h$  is a quadrilateral  $T = ABCD$ , as illustrated in Fig. 3.2. Consider the angle  $\phi := \angle DAB$ . Then either  $\phi \in (0, \theta_{\min})$  or  $\phi \in [\theta_{\min}, \pi)$ . We only have to treat the former case. Take  $E$  on the line through  $AB$  such that  $DE \perp AB$ , and  $F$  in the plane through  $OPQ$  such that  $DF$  is perpendicular to this plane. Hence,  $|DF| \leq |DE|$  holds and

$$\sin \phi = \frac{|DE|}{|AD|}.$$

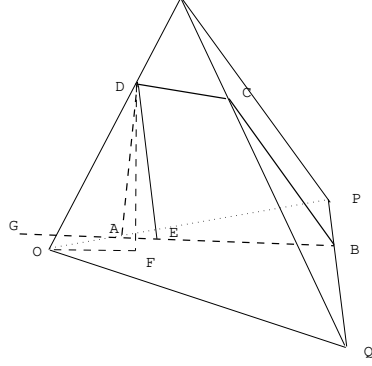


FIG. 3.2.

Furthermore, using  $\frac{|DF|}{|OD|} = \sin(\angle DOF) \geq \sin \theta_{\min}$  we get

$$\begin{aligned} \sin(\angle OAD) &= \frac{|OD|}{|AD|} \sin(\angle AOD) \leq \frac{|OD|}{|AD|} \leq \frac{1}{\sin \theta_{\min}} \frac{|DF|}{|AD|} \\ &\leq \frac{1}{\sin \theta_{\min}} \frac{|DE|}{|AD|} = \frac{\sin \phi}{\sin \theta_{\min}} < 1. \end{aligned}$$

This implies

$$\angle OAD \leq \arcsin\left(\frac{\sin \phi}{\sin \theta_{\min}}\right) \leq 2 \frac{\sin \phi}{\sin \theta_{\min}}.$$

Hence, since  $\angle DAB = \phi \leq 2 \sin \phi$ , we obtain

$$\angle OAB < \angle OAD + \angle DAB \leq \left(1 + \frac{1}{\sin \theta_{\min}}\right) 2 \sin \phi.$$

Using  $\angle OAB = \pi - \angle PAB$  and  $\angle PAB < \pi - \angle OPQ < \pi - \theta_{\min}$  results in

$$\theta_{\min} < \left(1 + \frac{1}{\sin \theta_{\min}}\right) 2 \sin \phi. \quad (3.6)$$

For  $\phi \in (0, \theta_{\min})$  the inequality (3.6) holds iff  $\phi \geq \phi_0$ , where  $\phi_0$  is the unique solution in  $(0, \frac{1}{2}\pi)$  of  $\theta_{\min} = \left(1 + \frac{1}{\sin \theta_{\min}}\right) 2 \sin \phi_0$ . Thus the result in b) holds.

□

The lemma readily yields the following result.

**THEOREM 3.2** (maximum angle condition). *Consider a regular family of tetrahedral triangulations  $\{\mathcal{T}_h\}_{h>0}$  and a surface triangulation  $\Gamma_h = \cup_{T \in \mathcal{F}_h} T$  that is consistent with  $\mathcal{T}_h$ . Assume that any quadrilateral element  $T = S \cap \Gamma_h$ ,  $S \in \mathcal{T}_h$ , is divided in two triangles by connecting the vertex with largest inner angle with its opposite vertex. The resulting surface triangulation satisfies the following maximal angle condition. There exists  $\phi_{\min} > 0$  depending only on  $\alpha$  from (3.1) such that:*

$$0 < \sup_{T \in \mathcal{F}_h} \phi_{i,T} \leq \pi - \phi_{\min} \quad i = 1, 2, 3, \quad (3.7)$$

where  $\phi_{i,T}$  are the inner angles of the element  $T$ .

*Proof.* If  $T = S \cap \Gamma_h$  is a triangle, then (3.7) directly follows from (3.3). Let  $T = S \cap \Gamma_h$  be a quadrilateral, with its four inner angles denoted by  $\theta_4 \geq \theta_3 \geq \theta_2 \geq$

$\theta_1 > 0$ . From the result in (3.4) we have  $\theta_i \geq \phi_{\min}$  for all  $i$ . The vertex with angle  $\theta_4$  is connected with the opposite vertex. Let  $T_1$  be one of the resulting triangles. One of the angles of  $T_1$  is  $\theta_j$  with  $j \in \{1, 2, 3\}$ . From  $\theta_j \geq \phi_{\min}$  it follows that the other two angles are both bounded by  $\pi - \phi_{\min}$ . Furthermore, from  $\theta_j = 2\pi - \theta_4 - \sum_{i=1, i \neq j}^3 \theta_i \leq 2\pi - \theta_j - 2\phi_{\min}$  it follows that  $\theta_j \leq \pi - \phi_{\min}$  holds.  $\square$

In the remainder we assume that quadrilaterals are subdivided in the way as explained in Theorem 3.2. Hence, the inner angles in the surface triangulation  $\mathcal{F}_h$  are bounded by a constant  $\theta^* < \pi$  that depends only on the stability (close to  $\Gamma$ ) of the outer tetrahedral triangulation  $\mathcal{T}_h$ . In particular  $\theta^*$  is *independent of  $h$  and of how  $\Gamma_h$  intersects the outer triangulation  $\mathcal{T}_h$* .

**4. Application in a finite element method.** In this section, we use the maximum angle property of the surface triangulation to derive an optimal finite element interpolation result. On  $\mathcal{F}_h$  we consider the space of linear finite element functions:

$$V_h = \{v_h \in \mathcal{C}(\Gamma_h) : v_h \in \mathcal{P}_1(T) \text{ for all } T \in \mathcal{F}_h\}. \quad (4.1)$$

This finite element space is the same as the one studied by Dziuk in [5], but an important difference is that in the approach in [5] the triangulations have to be shape regular. In general, the finite element space  $V_h$  is different from the surface finite element space constructed in [8, 9].

Below we derive an approximation result for the finite element space  $V_h$ . Since the discrete surface  $\Gamma_h$  varies with  $h$ , we have to explain in which sense  $\Gamma_h$  is close to  $\Gamma$ . For this we use a standard setting applied in the analysis of discretization methods for partial differential equations on surfaces, e.g. [4, 5, 6, 7, 9].

Let  $U := \{x \in \mathbb{R}^3 \mid \text{dist}(x, \Gamma) < c\}$  be a sufficiently small neighborhood of  $\Gamma$ . We define  $\mathcal{T}_h^\Gamma := \{T \in \mathcal{T}_h \mid \text{meas}_2(T \cap \Gamma_h) > 0\}$ , i.e., the collection of tetrahedra which intersect the discrete surface  $\Gamma_h$ , and assume that  $\mathcal{T}_h^\Gamma \subset U$ . Let  $d$  be the signed distance function to  $\Gamma$ , with  $d < 0$  in the interior of  $\Gamma$ ,

$$d : U \rightarrow \mathbb{R}, \quad |d(x)| := \text{dist}(x, \Gamma) \text{ for all } x \in U.$$

Thus  $\Gamma$  is the zero level set of  $d$ . Note that  $\mathbf{n}_\Gamma = \nabla d$  on  $\Gamma$ . We define  $\mathbf{n}(x) := \nabla d(x)$  for  $x \in U$ . Thus  $\mathbf{n}$  is the outward pointing normal on  $\Gamma$  and  $\|\mathbf{n}(x)\| = 1$  for all  $x \in U$ . Here and in the remainder  $\|\cdot\|$  denotes the Euclidean norm on  $\mathbb{R}^3$ . We introduce a local orthogonal coordinate system by using the projection  $\mathbf{p} : U \rightarrow \Gamma$ :

$$\mathbf{p}(x) = x - d(x)\mathbf{n}(x) \text{ for all } x \in U.$$

We assume that the decomposition  $x = \mathbf{p}(x) + d(x)\mathbf{n}(x)$  is unique for all  $x \in U$ . Note that  $\mathbf{n}(x) = \mathbf{n}(\mathbf{p}(x))$  for all  $x \in U$ . For a function  $v$  on  $\Gamma$ , its extension is defined as

$$v^e(x) := v(\mathbf{p}(x)), \text{ for all } x \in U. \quad (4.2)$$

The outward pointing (piecewise constant) unit normal on  $\Gamma_h$  is denoted by  $\mathbf{n}_h$ . Using this local coordinate system we introduce the following assumptions on  $\Gamma_h$ :

$$\mathbf{p} : \Gamma_h \rightarrow \Gamma \text{ is bijective,} \quad (4.3)$$

$$\max_{x \in \Gamma_h} |d(x)| \lesssim h^2, \quad (4.4)$$

$$\max_{x \in \Gamma_h} \|\mathbf{n}(x) - \mathbf{n}_h(x)\| \lesssim h, \quad (4.5)$$

where  $h = \sup_{T \in \mathcal{T}_h^\Gamma} \rho(T)$ . In (4.4)-(4.5) we use the common notation, that the inequality holds with a constant independent of  $h$ . In (4.5), only  $x \in \Gamma_h$  are considered for which  $\mathbf{n}_h(x)$  is well-defined. Using these assumptions, the following result is derived in [5].

LEMMA 4.1. *For any function  $u \in H^2(\Gamma)$ , we have, for arbitrary  $T \in \mathcal{F}_h$  and  $\tilde{T} := \mathbf{p}(T)$ :*

$$\|u^e\|_{0,T} \simeq \|u\|_{0,\tilde{T}}, \quad (4.6)$$

$$|u^e|_{1,T} \simeq |u|_{1,\tilde{T}}, \quad (4.7)$$

$$|u^e|_{2,T} \lesssim |u|_{2,\tilde{T}} + h|u|_{1,\tilde{T}}, \quad (4.8)$$

where  $A \simeq B$  means  $B \lesssim A \lesssim B$  and the constants in the inequalities are independent of  $T$  and of  $h$ .

**4.1. Finite element interpolation error.** Based on the results in Lemma 4.1, the maximum angle property and the approximation results derived in [1] we easily obtain an optimal bound for the interpolation error in the space  $V_h$ . Consider the standard finite element nodal interpolation  $I_h : C(\Gamma_h) \rightarrow V_h$ :

$$(I_h v)(x) = v(x), \quad \text{for all } x \in \mathcal{V}, \quad (4.9)$$

with  $\mathcal{V}$  the set of vertices of the triangles in  $\Gamma_h$ .

THEOREM 4.2. *For any  $u \in H^2(\Gamma)$  we have*

$$\|u^e - I_h u^e\|_{L^2(\Gamma_h)} \lesssim h^2 \|u\|_{H^2(\Gamma)}, \quad (4.10)$$

$$\|u^e - I_h u^e\|_{H^1(\Gamma_h)} \lesssim h \|u\|_{H^2(\Gamma)}. \quad (4.11)$$

*Proof.* From standard interpolation theory we have

$$\|u^e - I_h u^e\|_{L^2(T)} \lesssim h^2 |u^e|_{2,T},$$

where the constant in the upper bound is independent of (the shape of)  $T$ . Using the result in (4.8) and summing over  $T \in \mathcal{F}$  proves the result (4.10). For the interpolation error bound in the  $H^1$ -norm we use the results from [1]. For the interpolation error bounds derived in that paper the maximum angle property is essential. From [1] we get

$$\|u^e - I_h u^e\|_{H^1(T)} \lesssim h \|u\|_{H^2(T)}.$$

Due to the maximum angle property the constant in the upper bound is independent of  $T$ . Using the results in Lemma 4.1 and summing over  $T \in \mathcal{F}_h$  we obtain the result (4.11).  $\square$

If one considers an  $H^1(\Gamma)$  elliptic partial differential equation on  $\Gamma$ , the error for its finite element discretization in the surface space  $V_h$  can be analyzed along the same lines as in [5]. A difference with the planar case is that geometric errors arise due to the approximation of  $\Gamma$  by  $\Gamma_h$ . Using the interpolation error bounds in Theorem 4.2 and bounding the geometric errors, with the help of the assumptions (4.3)-(4.5), results in optimal order discretization error bounds.

**4.2. Conditioning of the mass matrix.** Clearly the (strong) shape irregularity of the surface triangulation will influence the conditioning of the mass and stiffness matrices. Let  $N$  be the number of vertices in the surface triangulation and  $\{\phi_i\}_{i=1}^N$  the nodal basis of the finite element space  $V_h$ . The mass and stiffness matrices are given by

$$\mathbf{M} = (m_{ij})_{i,j=1}^N, \quad \text{with} \quad m_{ij} = \int_{\Gamma_h} \phi_i \phi_j ds, \quad (4.12)$$

$$\mathbf{A} = (a_{ij})_{i,j=1}^N, \quad \text{with} \quad a_{ij} = \int_{\Gamma_h} \nabla_{\Gamma_h} \phi_i \nabla_{\Gamma_h} \phi_j ds. \quad (4.13)$$

We also need their scaled versions. Let  $\mathbf{D}_M$  and  $\mathbf{D}_A$  be the diagonals of  $\mathbf{M}$  and  $\mathbf{A}$ , respectively. The scaled matrices are denoted by

$$\mathbf{M}^s = \mathbf{D}_M^{-\frac{1}{2}} \mathbf{M} \mathbf{D}_M^{-\frac{1}{2}}, \quad \mathbf{A}^s = \mathbf{D}_A^{-\frac{1}{2}} \mathbf{A} \mathbf{D}_A^{-\frac{1}{2}}. \quad (4.14)$$

From a simple scaling argument it follows that the spectral condition number of  $\mathbf{M}^s$  is bounded uniformly in  $h$  and in the shape (ir)regularity of the surface triangulation. For completeness we include a proof.

**THEOREM 4.3.** *The following holds:*

$$\frac{2}{\sqrt{2}+2} \leq \frac{\langle \mathbf{M} \mathbf{v}, \mathbf{v} \rangle}{\langle \mathbf{D}_M \mathbf{v}, \mathbf{v} \rangle} \leq 4 \quad \text{for all } \mathbf{v} \in \mathbb{R}^N, \mathbf{v} \neq 0.$$

*Proof.* The set of all vertices in  $\mathcal{F}_h$  is denoted by  $\mathcal{V} = \{\xi_i \mid 1 \leq i \leq N\}$ . Let  $\mathbf{v} \in \mathbb{R}^N$  and  $v_h \in V_h$  be related by  $v_h = \sum_{i=1}^N v_i \phi_i$ , i.e.,  $v_i = v_h(\xi_i)$ . Consider a triangle  $T \in \mathcal{F}_h$  and let its three vertices be denoted by  $\xi_1, \xi_2, \xi_3$ . Using quadrature we obtain

$$\begin{aligned} \int_T v_h(s)^2 ds &= \frac{|T|}{3} \left( \frac{1}{4}(v_1 + v_2)^2 + \frac{1}{4}(v_2 + v_3)^2 + \frac{1}{4}(v_3 + v_1)^2 \right) \\ &= \frac{|T|}{6} (v_1^2 + v_2^2 + v_3^2 + v_1 v_2 + v_2 v_3 + v_3 v_1). \end{aligned}$$

Hence,  $\int_T v_h(s)^2 ds \leq \frac{|T|}{3} \sum_{i=1}^3 v_i^2$  holds. From a sign argument it follows that at least one of the three terms  $v_1 v_2$ ,  $v_2 v_3$  or  $v_3 v_1$  must be positive. Without loss of generality we can assume  $v_1 v_2 \geq 0$ . Using  $|v_2 v_3 + v_3 v_1| \leq \frac{1}{\sqrt{2}}(v_1^2 + v_2^2 + v_3^2)$  we get

$$\int_T v_h(s)^2 ds \geq \frac{|T|}{6} \left( v_1^2 + v_2^2 + v_3^2 - \frac{1}{\sqrt{2}}(v_1^2 + v_2^2 + v_3^2) \right) = \frac{|T|}{6(\sqrt{2}+2)} (v_1^2 + v_2^2 + v_3^2).$$

Note that  $\langle \mathbf{M} \mathbf{v}, \mathbf{v} \rangle = \int_{\Gamma_h} v_h(s)^2 ds = \sum_{T \in \mathcal{F}_h} \int_T v_h(s)^2 ds$ , and thus we obtain, with  $\mathcal{V}(T)$  the set of the three vertices of  $T$ ,

$$\frac{2}{\sqrt{2}+2} \frac{1}{12} \sum_{T \in \mathcal{F}_h} |T| \sum_{\xi \in \mathcal{V}(T)} v_h(\xi)^2 \leq \langle \mathbf{M} \mathbf{v}, \mathbf{v} \rangle \leq 4 \frac{1}{12} \sum_{T \in \mathcal{F}_h} |T| \sum_{\xi \in \mathcal{V}(T)} v_h(\xi)^2. \quad (4.15)$$

We observe that

$$\frac{1}{12} \sum_{T \in \mathcal{F}_h} |T| \sum_{\xi \in \mathcal{V}(T)} v_h(\xi)^2 = \frac{1}{12} \sum_{i=1}^N |\text{supp}(\phi_i)| v_i^2 \quad (4.16)$$



holds. From the definition of  $\mathbf{D}_M$  it follows that

$$\begin{aligned} \langle \mathbf{D}_M \mathbf{v}, \mathbf{v} \rangle &= \sum_{i=1}^N \int_{\Gamma_h} \phi_i^2 ds v_i^2 = \sum_{i=1}^N v_i^2 \sum_{T \in \text{supp}(\phi_i)} \int_T \phi_i^2 ds \\ &= \sum_{i=1}^N v_i^2 \sum_{T \in \text{supp}(\phi_i)} \frac{|T|}{12} = \frac{1}{12} \sum_{i=1}^N |\text{supp}(\phi_i)| v_i^2. \end{aligned} \quad (4.17)$$

Combination of the results in (4.15), (4.16) and (4.17) completes the proof.  $\square$

**4.3. Conditioning of the stiffness matrix.** We finally address the issue of conditioning of the diagonally scaled stiffness matrix  $\mathbf{A}^s$ , cf. (4.14). This matrix has a one dimensional kernel due to the constant nodal mode. Thus, we consider the effective condition number  $\text{cond}(\mathbf{A}^s) = \lambda_{\max}(\mathbf{A}^s)/\lambda_2(\mathbf{A}^s)$ , where  $\lambda_2$  is the minimal nonzero eigenvalue. We shall argue below that the condition number of  $\mathbf{A}^s$  can not be bounded in general by a constant dependent exclusively on  $\mathcal{T}_h$ , but not on  $\Gamma_h$ . Indeed, assume a smooth closed surface  $\Gamma$ , with  $|\Gamma| = 1$ , and a smooth function  $u$  defined on  $\Gamma$ , such that  $\|\nabla_{\Gamma} u\|_{L^2(\Gamma)} = \|u\|_{H^2(\Gamma)} = 1$ . Let  $\Gamma_h$  be the zero level of the piecewise linear Lagrange interpolant of the signed distance function to  $\Gamma$ . Denote  $u_h = I_h u^e$ , as in Theorem 4.2, and  $\mathbf{v} = (v_1, \dots, v_N)^T$  is the corresponding vector of nodal values. From the result in (4.11) we obtain

$$\langle \mathbf{A} \mathbf{v}, \mathbf{v} \rangle = \|\nabla_{\Gamma_h} u_h\|_{L^2(\Gamma_h)} = 1 + O(h). \quad (4.18)$$

On the other hand, if there is a node  $\xi$  in the volume triangulation  $\mathcal{T}_h$  such that  $\text{dist}(\xi, \Gamma_h) < \varepsilon \ll 1$ , then there can appear a triangle in  $\mathcal{F}_h$  with a minimal angle of  $O(\varepsilon)$ . This implies that there is a diagonal element in  $\mathbf{A}$  of order  $O(\varepsilon^{-1})$ . Without loss of generality we may assume  $A_{11} = O(\varepsilon^{-1})$  and  $v_1 = 1$ . Thus we get

$$\langle \mathbf{D}_A \mathbf{v}, \mathbf{v} \rangle \geq A_{11} v_1^2 = O(\varepsilon^{-1}). \quad (4.19)$$

Comparing (4.18) and (4.19) we conclude that  $\text{cond}(\mathbf{A}^s) \geq O(\varepsilon^{-1})$ , with  $\varepsilon \rightarrow 0$ . Results of numerical experiments in the next section demonstrate that the blow up of  $\text{cond}(\mathbf{A}^s)$  can be seen in some cases.

One might also be interested in a more general dependence of the eigenvalues of  $\mathbf{A}^s$  on the distribution of tetrahedral nodes in  $\mathcal{T}_h$  in a neighborhood of  $\Gamma_h$ . To a certain extend this question is addressed in [8].

**5. Numerical experiment.** In this section we present a few results of numerical experiments which illustrate the interpolation estimates from Theorem 4.2 and the conditioning of mass and stiffness matrices. Assume the surface  $\Gamma$ , which is the unit sphere  $\Gamma = \{x \in \mathbb{R}^3 \mid \|x\| = 1\}$ , is embedded in the bulk domain  $\Omega = [-2, 2]^3$ . The signed distance function to  $\Gamma$  is denoted by  $d$ . We construct a hierarchy of uniform tetrahedral triangulations  $\{\mathcal{T}_h\}$  for  $\Omega$ , with  $h \in \{1/2, 1/4, 1/8, 1/16, 1/32\}$ . Let  $d_h$  be the piecewise nodal Lagrangian interpolant of  $d$ . The triangulated surface is given by

$$\Gamma_h = \bigcup_{T \in \mathcal{F}_h} T = \{x \in \Omega \mid d_h(x) = 0\}.$$

The corresponding finite element space  $V_h$  consists of all piecewise affine functions with respect to  $\mathcal{F}_h$ , as defined in (4.1). For  $h \in \{1/2, 1/4, 1/8, 1/16, 1/32\}$ , the resulting

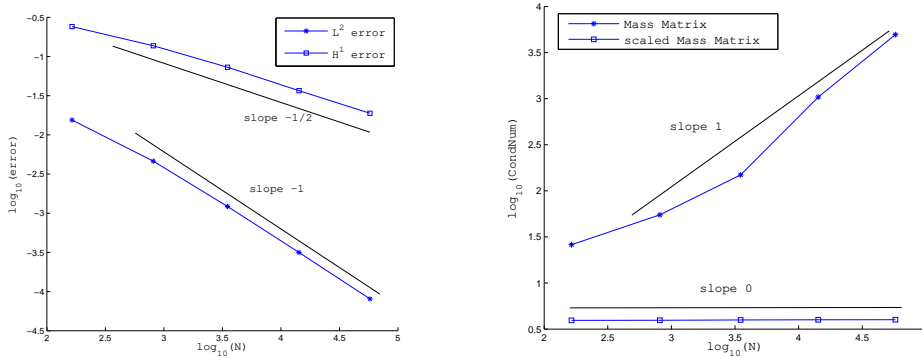


FIG. 5.1. Left: Interpolation error as a function of # d.o.f.; Right: The condition number of the mass matrix as a function of # d.o.f.

dimensions of  $V_h$  are  $N = 164, 812, 3500, 14264, 57632$ , respectively. In agreement with the 2D nature of  $\Gamma_h$ , we have  $N \sim h^{-2}$ .

To illustrate the result of Theorem 4.2, we present the interpolation errors  $\|u^e - I_h u^e\|_{L^2(\Gamma_h)}$  and  $|u^e - I_h u^e|_{1,\Gamma_h}$  for the smooth function

$$u(x) = \frac{1}{\pi} x_1 x_2 \arctan(2x_3)$$

defined on the unit sphere, with  $x = (x_1, x_2, x_3)^T$ . The dependence of the interpolation errors on the number of degrees of freedom  $N$  is shown in Figure 5.1 (left). We observe the optimal error reduction behavior, consistent with the estimates in (4.10), (4.11).

Further, for the same sequence of meshes we compute the spectral condition numbers of the mass matrix  $\mathbf{M}$  and the diagonally scaled mass matrix  $\mathbf{M}^s$ . The dependence of the condition numbers on the number of degrees of freedom  $N$  is illustrated in Figure 5.1 (right). As was proved in Theorem 4.3, the scaled mass matrix has a uniformly bounded condition number.

We discussed in section 4.3 that concerning the effective condition number of the scaled stiffness matrix the situation is more delicate. To illustrate this, we performed an experiment in which the intersection between a fixed outer triangulation and the surface is varied. Let  $\Gamma$  be the boundary of the unit sphere with the center located in  $(0, 0, z_c)$ . The discrete surface  $\Gamma_h$  is defined as described above, induced by the uniform outer triangulation. We choose a fixed outer triangulation with  $h = 1/16$ . We now consider different values for  $z_c$ , thus “moving the surface through the outer triangulation”. The  $z_c$  values are given in the first column of Table 5.1. Note that for the largest shift  $z_c = 0.03$  we have  $z_c \approx 0.5h$ .

For the different surface triangulations we computed the interpolation errors as described above. It turns out that for the values  $z_c \neq 0$  the error behavior is essentially the same as that for  $z_c = 0$  (illustrated in Fig. 5.1).

In the second to fourth columns of Table 5.1 two geometry related quantities are given. The second column shows the value of the maximum angle occurring in the surface triangulation. Consistent to the theory, cf. Theorem 3.2, the maximum angle is bounded away from  $180^\circ$ . Small angles, however, can occur. In the third and fourth column we show the value of the minimum angle and the number of

triangles in the surface triangulation with the smallest angle smaller than  $1^\circ$ . As expected, both the minimal angle and this number of small angles strongly varies depending on  $z_c$ . For  $z_c = 0$  the smallest angle in the surface triangulation has value  $\phi_{\min} = 1.85^\circ$ . Extremely small angles can occur, e.g. for  $z_c = 0.00005$ , we have  $\phi_{\min} = 8.54e-7^\circ$ . The dimension and the effective condition number of the scaled stiffness matrix  $\mathbf{A}^s$  are given in the fifth and sixth column of Table 5.1. The values of the condition number show a strong dependence on the sphere location (value of  $z_c$ ). These large condition numbers indicate that linear systems with these matrices may be hard to solve using an iterative method. To investigate this further, we used the standard PCG MATLAB solver with ILU(0) preconditioner. For given  $\mathbf{v}$ , we computed  $\mathbf{b} = \mathbf{A}^s \mathbf{v}$  and applied the MATLAB PCG iterative solver with a relative residual tolerance of  $10^{-8}$ . The resulting iteration numbers are given in column 7 of Table 5.1. These iteration counts are “high” compared to the ones that are generally needed for standard discretization of diffusion problems. To make this more quantitative, we constructed a reference matrix  $\mathbf{A}^{\text{ref}}$  as follows:  $\mathbf{A}^{\text{ref}} = \text{blocktridiag}(-\mathbf{B}^T, \mathbf{D}, -\mathbf{B})$ , with  $\mathbf{D} = \text{tridiag}(-1, 6, -1)$ ,  $\mathbf{B} = \text{tridiag}(0, 1, 1)$ . In most rows the matrix  $\mathbf{A}^{\text{ref}}$  has 7 nonzero entries, which is approximately the same as the average number of nonzero entries per row in the matrix  $\mathbf{A}^s$  used in the experiment. In  $\mathbf{A}^{\text{ref}}$  we use 120 blockrows and blockcolumns and the matrices  $\mathbf{D}$  and  $\mathbf{B}$  have dimension 120. Then the matrix  $\mathbf{A}^{\text{ref}}$  has dimension 14400, which is comparable to the dimension of  $\mathbf{A}^s$  used in the experiment, cf. Table 5.1. The same iterative solver with the same stopping criterion applied to a linear system with  $\mathbf{A}^{\text{ref}}$  resulted in 42 PCG iterations, which is much lower than the iteration numbers listed in Table 5.1.

In view of these observations, and the fact that solving a PDE on a surface (in 3D) is a *two*-dimensional problem, it is better to use a direct solver. We performed experiments with the MATLAB sparse direct solver  $\mathbf{A}^s \setminus \mathbf{b}$ . We measured computing time by the MATLAB function CPUTIME. For the system with the reference matrix  $\mathbf{A}^{\text{ref}}$  we obtained (on our machine) CPUTIME= 1.38. For the matrix  $\mathbf{A}^s$  we obtained CPU time measurements given in the last column of Table 5.1. These show that for the direct MATLAB solver the matrices  $\mathbf{A}^s$  are not (much) more difficult to deal with than the reference matrix  $\mathbf{A}^{\text{ref}}$ . Variations in CPU times are probably caused by slightly different fill-in properties of matrices for different grids. The one dimensional kernel of the matrix  $\mathbf{A}^s$  did not cause difficulties for the solver. We checked the accuracy of the computed solution (in the energy norm) and this was satisfactory.

$z_c$	$\phi_{\max}$	$\phi_{\min}$	#T: $\phi_{\min} < 1^\circ$	dim( $\mathbf{A}^s$ )	cond( $\mathbf{A}^s$ )	# PCG	CPUTIME
0.03	147.4°	0.050°	420	14406	1.82e+4	245	3.64
0.02	145.3°	0.027°	292	14376	2.20e+4	282	3.52
0.008	145.4°	0.014°	270	14368	3.44e+4	331	3.61
0.002	144.3°	0.002°	126	14300	1.94e+5	285	2.33
0.0005	141.0°	1.22e-4°	20	14288	3.07e+6	259	1.93
0.00025	140.4°	3.05e-5°	20	14288	1.23e+7	191	2.22
0.00005	139.9°	8.54e-7°	24	14288	3.06e+8	202	1.43
0	139.8°	1.85°	0	14264	9.14e+3	142	2.85

TABLE 5.1

Angles in the surface triangulation, dimension of  $\mathbf{A}^s$ , cond( $\mathbf{A}^s$ ), iteration count for PCG and timing for direct solver.

**6. Conclusions.** The main new result of this paper is a geometric property of the piecewise planar surface which is the zero level of a continuous piecewise affine

level set function. If this piecewise planar surface is consistent with an outer tetrahedral triangulation that satisfies the *minimum angle condition*, then after a suitable subdivision of the quadrilaterals into two triangles the resulting surface triangulation satisfies a *maximum angle condition*. This maximum angle property of the surface triangulation is used to derive optimal error bounds for the nodal interpolation operator in the finite element space of continuous piecewise linear functions on the surface triangulation. This implies that the discretization of a surface diffusion PDE in this finite element space results in optimal discretization error bounds. We study the conditioning of the scaled mass and stiffness matrices corresponding to this finite element space. The condition number of the scaled mass matrix is shown to be uniformly bounded. The scaled stiffness matrix can have a very large effective condition number. Results of a numerical experiment indicate that for solving systems with the scaled stiffness matrix it is better to use a sparse direct solver rather than an iterative solver. A topic that we plan to investigate further is whether some grid smoothing (elimination of extremely small angles) can be developed such that the optimal approximation property still holds and the conditioning of the scaled stiffness matrix is improved.

**Acknowledgments.** The authors thank the referees for their comments, which have led to significant improvements of the original version of this paper. This work has been supported in part by the DFG through grant RE1461/4-1 and the Russian Foundation for Basic Research through grants 12-01-91330, 12-01-00283.

#### REFERENCES

- [1] I. Babuška and A. K. Aziz. On the angle condition in the finite element method. *SIAM J. Numer. Anal.*, 13:214–226, 1976.
- [2] P. Ciarlet. *The Finite Element Method for Elliptic Problems*. North-Holland, Amsterdam, 1978.
- [3] A. Demlow. Higher-order finite element methods and pointwise error estimates for elliptic problems on surfaces. *SIAM J. Numer. Anal.*, 47:805–827, 2009.
- [4] A. Demlow and G. Dziuk. An adaptive finite element method for the Laplace-Beltrami operator on implicitly defined surfaces. *SIAM J. Numer. Anal.*, 45:421–442, 2007.
- [5] G. Dziuk. Finite elements for the Beltrami operator on arbitrary surfaces. In S. Hildebrandt and R. Leis, editors, *Partial differential equations and calculus of variations*, volume 1357 of *Lecture Notes in Mathematics*, pages 142–155. Springer, 1988.
- [6] G. Dziuk and C. Elliott. Finite elements on evolving surfaces. *IMA J. Numer. Anal.*, 27:262–292, 2007.
- [7] G. Dziuk and C. Elliott.  $L^2$ -estimates for the evolving surface finite element method. *Math. Comp.*, 82:1–24, 2013.
- [8] M. A. Olshanskii and A. Reusken. A finite element method for surface PDEs: matrix properties. *Numer. Math.*, 114:491–520, 2009.
- [9] M. A. Olshanskii, A. Reusken, and J. Grande. A finite element method for elliptic equations on surfaces. *SIAM J. Numer. Anal.*, 47:3339–3358, 2009.
- [10] J.-J. Xu and H.-K. Zhao. An Eulerian formulation for solving partial differential equations along a moving interface. *J. Sci. Comput.*, 19:573–594, 2003.